Supporting Information

Carvalho et al. 10.1073/pnas.1408224111

SI Materials and Methods

Western Immunoblot Analysis. Twenty embryos (stage 15–16; w^{1118} and *Dif dl*) were homogenized in 2× Laemmli sample buffer, and extracted protein samples were separated on a 10% (wt/vol) SDS/PAGE, and transferred to a nitrocellulose membrane (Bio-Rad). Blots were developed using Amersham ECL Plus Western Blotting Detection System (GE Healthcare Life Sciences). Rat E-cadherin antibody (DCAD2, DSHB) was used at 1:50 dilution; mouse α-tubulin (clone DM1A, T6199, Sigma-Aldrich) was diluted 1:10,000.

Bands were detected using the Chemidoc Imaging System (Bio-Rad) and quantified with the Fiji software, Gels plug-in. Intensity profiles of E-cadherin bands were normalized against α-tubulin bands in five paired blots (w^{1118} and *Dif dl* collected on the same day).

Quantitative PCR. Wild-type (w^{1118}) and *Dif dl* embryos at stage 15–16 were collected and dechorionated. RNA was extracted from 100 embryos of each genotype by using the RNeasy Plus Micro Kit (Qiagen). Total RNA (0.5 μg) was reverse-transcribed with the Transcriptor High Fidelity cDNA Synthesis kit (Roche). Quantitative PCR (Q-PCR) was performed by using the Fast Green Master Mix (Roche) and the Roche LightCycler 480. Gene expression amounts were normalized to *RpL32* gene; the ΔΔCT method (1) was used to calculate fold change. Three biological replicates were analyzed, each with four technical replicates. A two-tailed, paired Wilcoxon nonparametric test was performed to assay significant differences between wild type and *Dif dl* ΔCT values. Primers were the following:

RpL32 F-5′-CACCAAGCACTTCATCCGCCACCAGTC-3′;

RpL32 R-5′-CGGTTCTGCATGAGCAGGACCTCCA-3′;

shg F-5′-AAGAACGACCACAAGCCGCACTTCCA-3′;

shg R-5′-TCCATCGAACGCACGCACCTTCAGC-3′.

1. Livak KJ, Schmittgen TD (2001) Analysis of relative gene expression data using real-time quantitative PCR and the 2(-Delta Delta C(T)) Method. *Methods* 25(4):402–408.

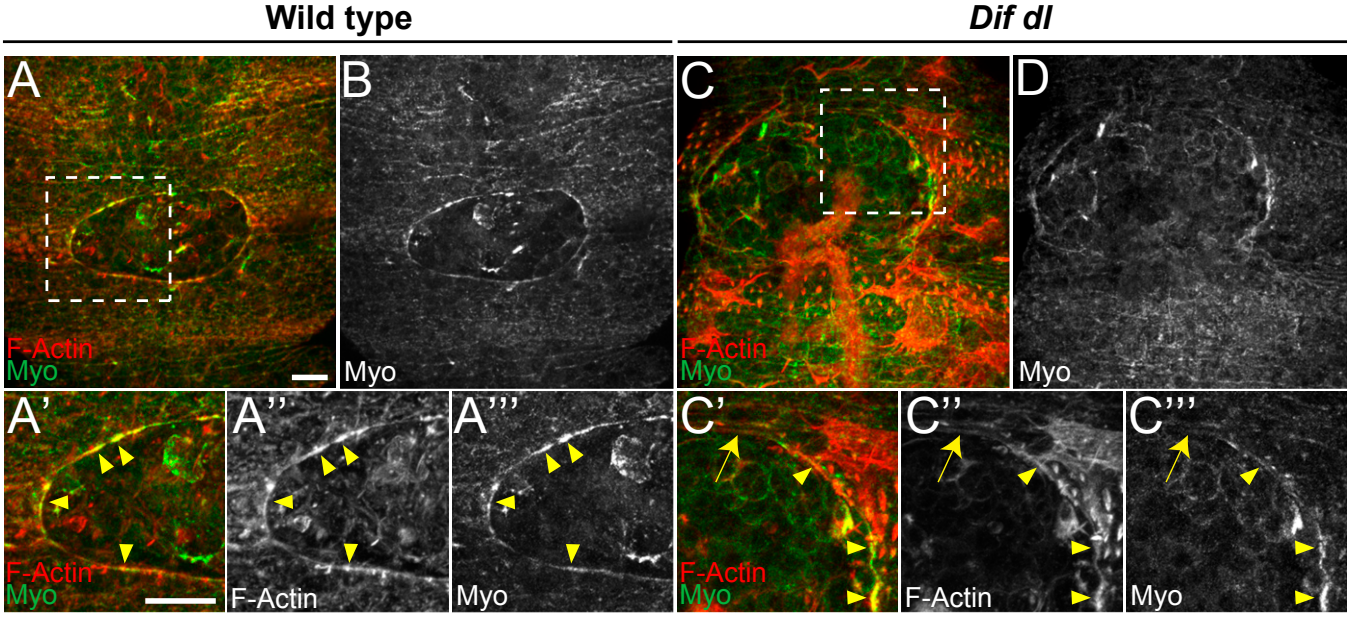

Fig. S1. Related to Fig. 2: In wounded *Dif dl* embryos, Myosin II is at the wound margin only in cells that had built an actin cable. (*A–D*) At 1 h after wounding, embryos of stage 15 were stained with GFP antibody to label the nonmuscle Myosin II Regulatory Light Chain fusion to GFP (Sgh::GFP) and with phalloidin to outline F-actin in epidermal cells. *A–C* represent merged images, whereas *B* and *D* show only Sgh::GFP (Myo). Images were acquired with identical settings. The areas for the close-ups (*A′–C‴*) are shown in *A* and *C*. Myosin II and F-actin are detected along the wound edge simultaneously at 5 min after ablation (1). The Sqh::GFP chimera fully complements a null *sgh* allele and is therefore functional (2). (*A–B*) In wild type ($n = 13$), epidermal cells show a continuous actin cable along the wound margin (*A*). Myosin II (*B*) overlaps tightly in localization with F-actin (compare *A″* to *A‴*). (*C–D*) In *Dif dl* mutants ($n = 13$), epidermal cells show a discontinuous actin cable along the wound margin (*C*). Cells that have built some actin cable (*C′* and *C″* arrowheads) localize Myosin II to the wound edge (compare *C″* to *C‴*). By contrast, cells that lack actin cable (*C′* and *C″*, arrow) fail to show Myosin II at the wound edge (compare *C″* to *C‴*). All images are the maximum z projections of 20.8- to 23.6-μm stacks (52–59 slices). (Scale bars: 10 μm.)

1. Abreu-Blanco MT, Verboon JM, Liu R, Watts JJ, Parkhurst SM (2012) *Drosophila* embryos close epithelial wounds using a combination of cellular protrusions and an actomyosin purse string. *J Cell Sci* 125(Pt 24):5984–5997.
2. Royou A, Field C, Sisson JC, Sullivan W, Karess R (2004) Reassessing the role and dynamics of nonmuscle myosin II during furrow formation in early *Drosophila* embryos. *Mol Biol Cell* 15(2):838–850.

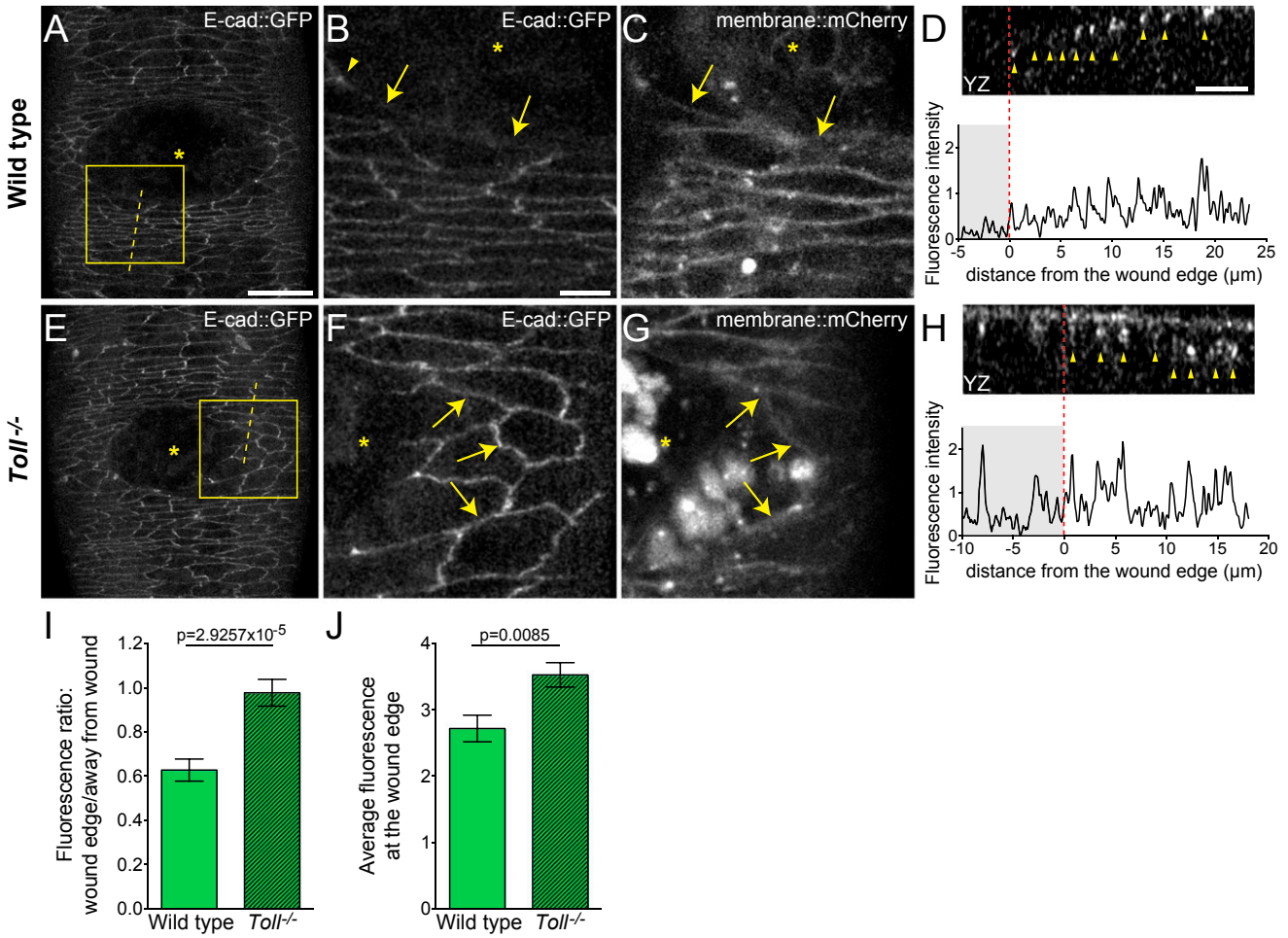

Fig. S2. Related to Fig. 3: Remodeling of E-cad::GFP at the wound edge is impaired in *Toll*$^{-/-}$ mutants. (*A*–*H*) Ventral epidermis of embryos at stage 15 expressing E-cad::GFP and membrane::mCherry. (*A*, *B*, and *E*–*H*) show E-cad::GFP, whereas (*C* and *G*) show membrane::mCherry. Images are taken with identical settings at 5 min after wounding of wild type (*A*–*D*) and *Toll*$^{-/-}$ (*E*–*H*). (*B*, *C*, *F*, and *G*) are high-magnification images of the wound edge in wild-type and *Toll*$^{-/-}$ embryos (boxed regions in *A* and *E*). The transallelic combination used in this experiment was *Toll*^{9QRE}/*Toll*$^{1\text{-}RXA}$. In wild type, wound-edge membranes have low levels of E-cad::GFP (*A*; *B*, arrows) compared with cellular junctions at a distance from the wound. In some wound-edge cells, E-cad::GFP becomes enriched in apical puncta (*B*, arrowhead) at contact points between the cells. In *Toll*$^{-/-}$, all epidermal cells, at the wound edge and far from the wound, have high levels of E-cadherin (*E*; *F*, arrows). Wound-edge membranes are marked with membrane::mCherry (*C* and *G*). Asterisks show the center of the wound. (*D* and *H*) YZ cross-sections of the epidermis (apical side is up). Dashed lines in *A* and *E* mark the positions of the cross-sections. The graphs show the fluorescence intensity profiles of E-cad::GFP in these YZ cross-sections. The wound area is shaded; the wound margin is marked with a red dashed line. Both wild-type and *Toll*$^{-/-}$ embryos display apical localization of E-cad::GFP (arrowheads in *D* and *H*). Wild-type cells have low levels of E-cad::GFP at the wound edge, whereas *Toll*$^{-/-}$ cells retain higher levels of fluorescence. (Scale bars: *A* and *E*, 20 μm; *B*–*D* and *F*–*H*, 5 μm.) (*I*) Ratio of E-cad::GFP at wound-edge membranes versus E-cad::GFP at AJs away from the wound in wild type and in *Toll*$^{-/-}$. In wild type, this ratio is significantly lower (0.627 ± 0.050) than in *Toll*$^{-/-}$ (0.977 ± 0.060), $P = 2.93 \times 10^{-5}$ (Mann–Whitney test). Error bars are SEM. Measurements of 68 junctions in five wild-type embryos and 99 junctions in six *Toll*$^{-/-}$ embryos were used for this graph. (*J*) E-cad::GFP fluorescence intensity at the membrane surrounding the wound in wild type and in *Toll*$^{-/-}$. Compared with wild type, *Toll*$^{-/-}$ embryos show significantly higher E-cad::GFP fluorescence ($P = 0.0085$, Mann–Whitney test). The value in *Toll*$^{-/-}$ (3.53 ± 0.184) is approximately 1.3-fold higher than in wild type (2.72 ± 0.201). Measurements of 68 wound-edge membranes from five wild-type embryos and 99 wound-edge membranes from six *Toll*$^{-/-}$ embryos are plotted. Error bars represent SEM.

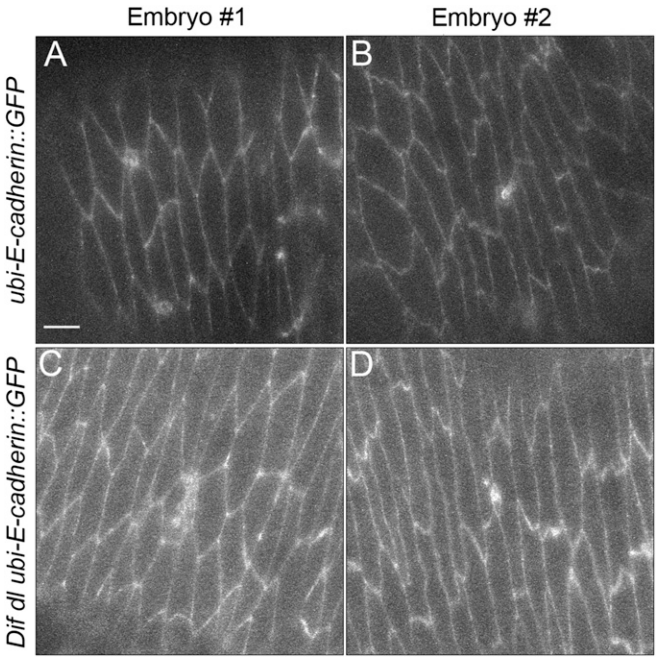

Fig. S3. Related to Fig. 4: *Dif dl* unwounded embryos have high *E-cad::GFP* fluorescence levels. Live embryos were imaged with identical settings. Images are the maximum *z* projections of a 3-μm stack (three slices). (Scale bar: 5 μm.) *A* and *B* show the ventral-lateral epidermis of two different unwounded control embryos of the genotype *ubi-E-cad::GFP/+*. *C* and *D* show the ventral-lateral epidermis of two different unwounded *Dif dl* mutants of the genotype *Dif dl ubi-E-cad::GFP/Dif dl +*. The mean gray value of a single cell-to-cell interface (subsequently photobleached) was measured in each embryo by using Fiji. Quantifications of E-cad::GFP showed that wild-type embryos ($n = 16$) have significantly lower fluorescence than *Dif dl* mutants ($n = 16$), $P < 0.05$ (Student's *t* test).

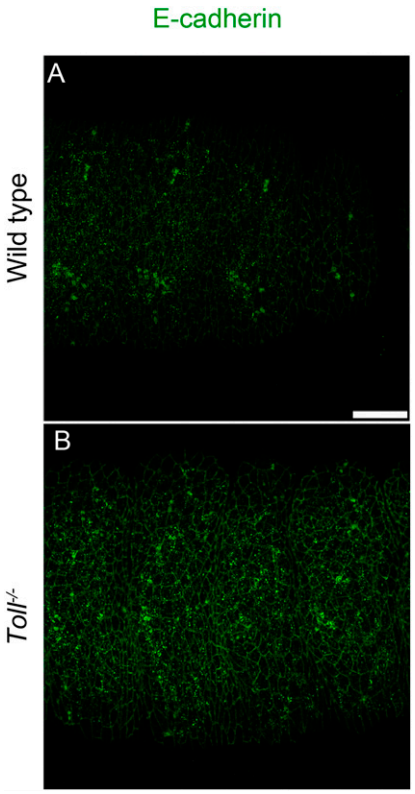

Fig. S4. Related to Fig. 4: $Toll^{-/-}$ unwounded embryos have high endogenous E-cadherin expression. Embryos were fixed and stained with E-cad antibody. Five embryos of each genotype were imaged with identical settings. Images are the maximum *z* projections of a 19.6-μm stack (49 slices). (*A*) Intact wild-type embryo (w^{1118}). (*B*) Intact $Toll^{-/-}$ embryo. (Scale bar: 20 μm.)

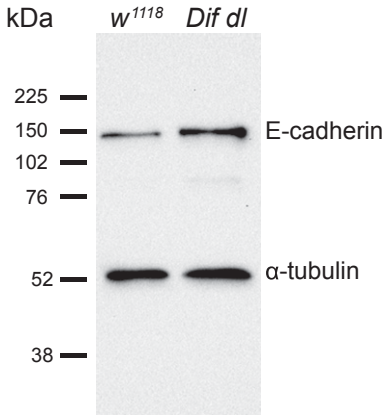

Fig. S5. Related to Fig. 4: Western immunoblot analysis of E-cad protein levels in unwounded *Dif dl* embryos. Uncropped Western blot of protein extracts from intact w^{1118} and *Dif dl* embryos at stages 15 and 16. The blot was probed with E-cad antibody and with α-tubulin antibody, which served as a loading control. Protein molecular mass markers are indicated on the left edge of the membrane. Measurements of five independently collected paired samples (w^{1118} and *Dif dl*) indicated that *Dif dl* embryos have on average 70% (1.7-fold) more E-cad relative to the controls.

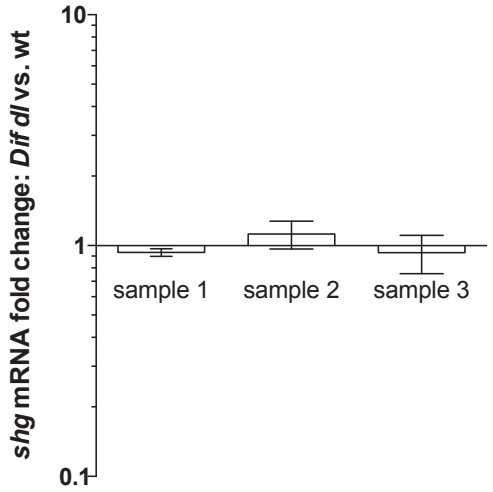

Fig. S6. Related to Fig. 6: Q-PCR of *shg* mRNA in unwounded *Dif dl* embryos. The graph represents Q-PCR results performed on three biological replicates. Each error bar in each column represents the SD from four technical replicates. The results showed that the amount of *shg* RNA in unwounded *Dif dl* embryos (stages 15–16) is not significantly different from the controls (w^{1118}); $P = 0.8486$ in paired Wilcoxon nonparametric test.

Table S1. *dorsal::GFP* rescues lethality of *Dif dl* double mutants, related to Fig. 5

Genotype	Sample size, *n*	Survival to adulthood, %
Dif dl	403	9.35
Dif dl; *dl::GFP*/+	523	179

To determine survival to adulthood in percents, the number of *Dif dl* mutants that survived to adulthood was compared with the number of *Dif dl*/*CyO-CTG* heterozygous siblings from the same cross (defined as 100%). Similarly, in the rescue experiment the number of *Dif dl* mutants that carried *dl::GFP* was compared with the number of *Dif dl*/*CyO-CTG; dl::GFP*/*MKRS* heterozygous siblings from the same cross (defined as 100%). The rescue exceeds 100% because the heterozygous siblings carry two balancer chromosomes and are not very healthy.

Table S2. *dorsal::GFP* rescues the wound-repair phenotype of *Dif dl* embryos, related to Fig. 5

Genotype	Sample size, *n*	Embryos with open wounds, %
w^{1118}	157	7.5
Dif dl	87	65.3
Dif dl; *dl::GFP/MKRS*	36	25

Dif dl embryos have a higher rate of open wounds (65.3%) compared with the controls (7.5%). The percentage of open wounds is reduced to 25% when *Dif dl* mutants expressed a *dl::GFP* transgene under the control of the *dl* promoter. Therefore, *dl::GFP* rescued the wound-repair phenotype of *Dif dl* embryos but not fully. The wounded embryos were of the genotype: *Dif dl; dl::GFP/MKRS*. The presence of a balancer chromosome could have contributed to the less efficient repair. Alternatively, under conditions of injury, Dorsal::GFP does not perform as well as the endogenous protein.

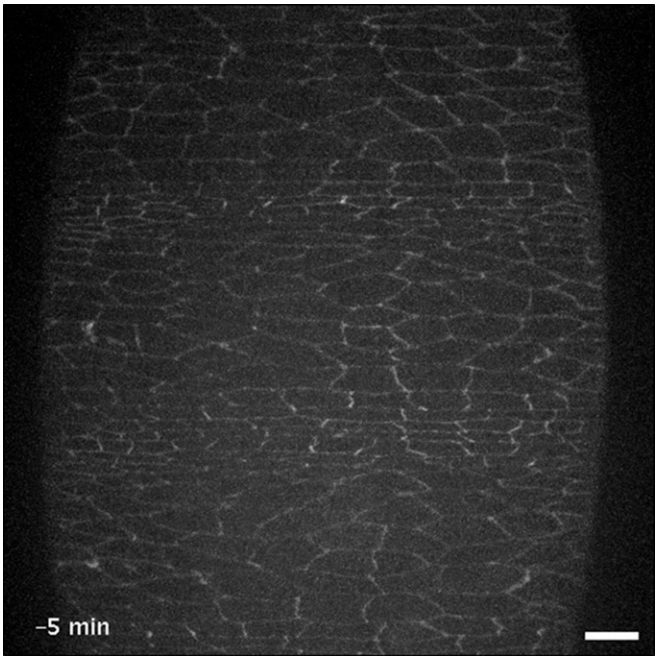

Movie S1. E-cad::GFP dynamics during epithelial wound closure. Time-lapse imaging of wound closure in the ventral epidermis of an embryo at stage 15 expressing *ubi-E-cad::GFP*. Immediately after wounding E-cad::GFP decreases at the membranes of epidermal cells facing the wound. This event is followed by the formation of E-cad::GFP foci in the lateral planes of the wound-edge cells that are clearly seen in this video at 10 min postwounding. Images are the maximum *z*-projections of an 18-μm stack (49 slices) and were captured every 5 min on an Andor Revolution Spinning Disk Confocal Microscope. The first frame shows the embryo before wounding. (Scale bar: 10 μm.)

Movie S1

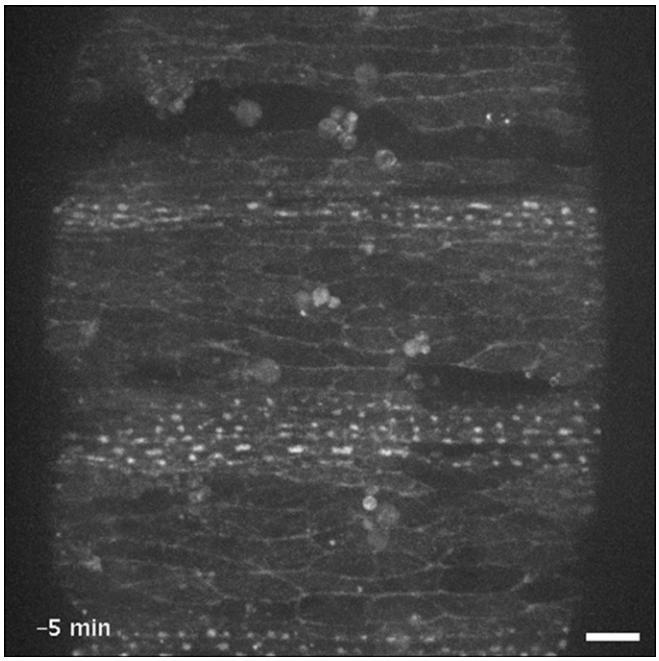

Movie S2. F-Actin dynamics during epithelial wound closure. This is the same embryo as in Movie S1, which in addition to *ubi-E-cad::GFP* also expresses *UAS-CherryFP::Moesin* under the control of *e22c-Gal4* (*e22c* > *Cherry::Moesin*). Actin-cable formation occurs between 5 and 15 min after wounding. Thus, the assembly of the actin cable starts after the E-cad::GFP is down-regulated at the wound-edge margin. Images are the maximum z projections of an 18-μm stack (49 slices) and were captured every 5 min on an Andor Revolution Spinning Disk Confocal Microscope. First frame shows the embryo before wounding. (Scale bar: 10 μm.)

Movie S2

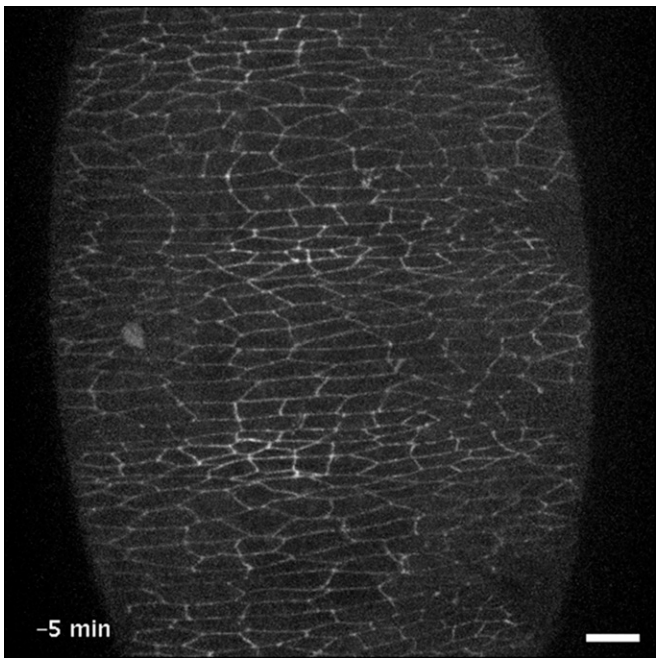

Movie S3. E-cad::GFP dynamics in wounded *Dif dl* embryos. Time-lapse imaging of the ventral epidermis of a *Dif dl* embryo at stage 15 expressing *ubi-E-cad::GFP*. Before laser ablation, E-cad::GFP is strongly expressed at the apical junctions of all epidermal cells. Upon ablation, wound-edge epidermal cells continue to maintain high apical E-cad::GFP (left side of the wound). Images are the maximum *z* projections of an 18-μm stack (49 slices) and were captured every 5 min on an Andor Revolution Spinning Disk Confocal Microscope. First frame shows the embryo before wounding. (Scale bar: 10 μm.)

Movie S3

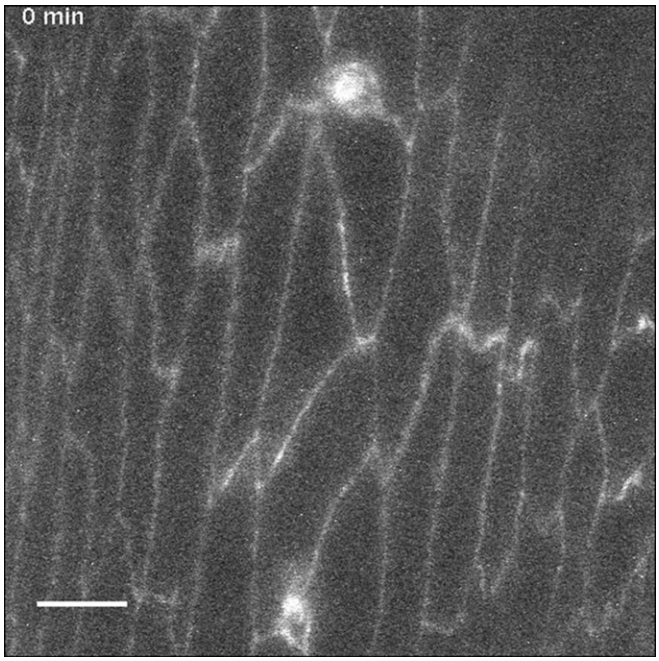

Movie S4. FRAP in wild-type embryos. E-cad::GFP recovers rapidly after photobleaching of the cell interface in the ventral-lateral epidermis of a wild-type embryo (*ubi-E-cad::GFP*/+). Images are the maximum *z* projections of the entire 3-μm stack (three slices). Images were captured every minute on a Zeiss LSM 510 META confocal microscope. The first frame shows the embryo before bleaching. (Scale bar: 5 μm.)

Movie S4

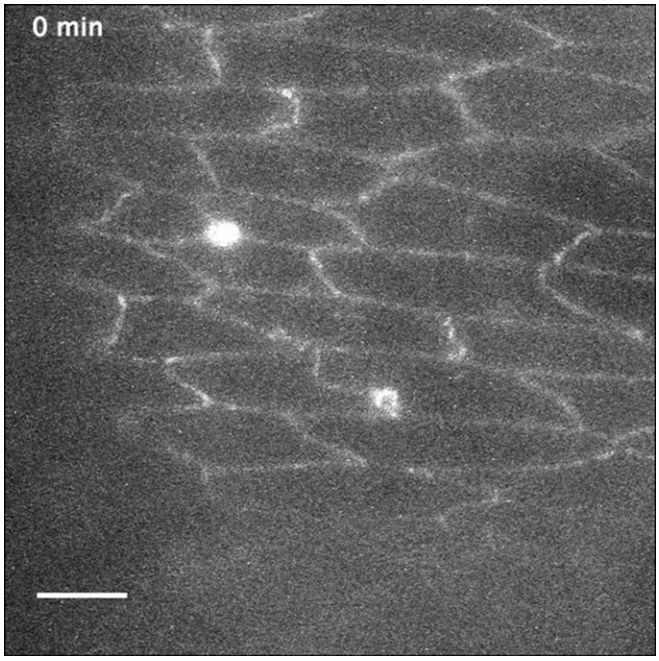

Movie S5. FRAP in *Dif dl* embryos. E-cad::GFP does not recover at all after photobleaching of cell interfaces in the ventral-lateral epidermis of this *Dif dl* embryo. Images are the maximum *z* projections of the entire 3-μm stack (three slices). Images were captured every minute on a Zeiss LSM 510 META confocal microscope. The first frame shows the embryo before bleaching. (Scale bar: 5 μm.)

Movie S5

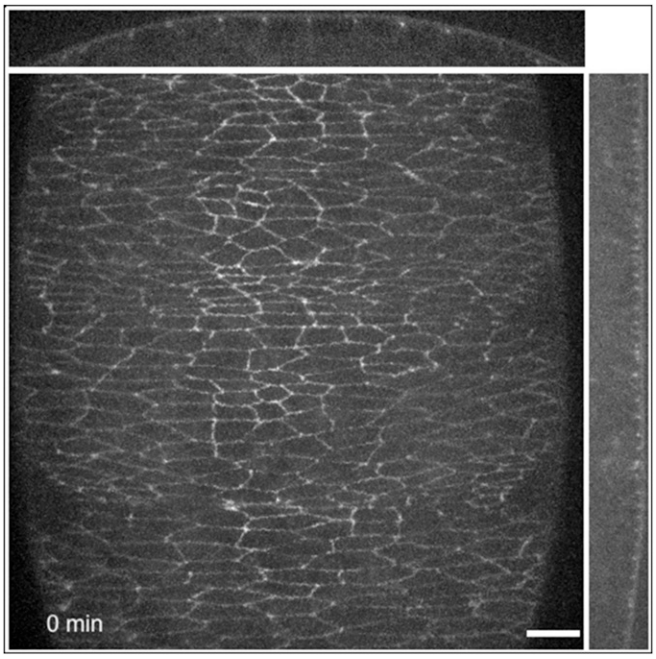

Movie S6. Dynamics of E-cad::GFP and Dorsal::GFP during epithelial wound closure. Time-lapse imaging of the ventral epidermis of a wild-type embryo at stage 15 expressing simultaneously *ubi-E-cad::GFP* and *dorsal::GFP*. Before laser ablation, E-cad::GFP is localized at the apical junctions of all epidermal cells whereas Dorsal::GFP is excluded from the nuclei. Upon wounding, wound-edge membranes show immediate decrease in E-cad::GFP while Dorsal::GFP undergoes a more gradual translocation to the epidermal nuclei. Cells around the wound edge that have high levels of nuclear Dorsal::GFP show little junctional E-cad::GFP. In contrast, cells without prominent nuclear Dorsal::GFP show high junctional E-cad::GFP fluorescence. The left panel is the maximum *z*-projection of an 18-μm stack (49 slices); top panel shows a single XZ slice and right panel shows a single YZ slice. Images were captured every 5 min on an Andor Revolution Spinning Disk Confocal Microscope. First frame shows the embryo before wounding. (Scale bar: 10 μm.)

Movie S6